PHYSICAL REVIEW E VOLUME 56, NUMBER 4 OCTOBER 1997

# Real-time experimental control of a system in its chaotic and nonchaotic regimes

David J. Christini,[1] Visarath In,[2] Mark L. Spano,[2] William L. Ditto,[3] and James J. Collins[1]
[1]Department of Biomedical Engineering, Boston University, 44 Cummington Street, Boston, Massachusetts 02215
[2]Naval Surface Warfare Center, Carderock Division, West Bethesda, Maryland 20817
[3]Applied Chaos Laboratory, School of Physics, Georgia Institute of Technology, Atlanta, Georgia 30332

(Received 1 July 1997)

Current model-independent control techniques are limited, from a practical standpoint, by their dependence on a precontrol learning stage. Here we use a real-time, adaptive, model-independent (RTAMI) feedback control technique to control an experimental system — a driven magnetoelastic ribbon — in its nonchaotic and chaotic regimes. We show that the RTAMI technique is capable of tracking and stabilizing higher-order unstable periodic orbits. These results demonstrate that the RTAMI technique is practical for on-the-fly (i.e., no learning stage) control of real-world dynamical systems. [S1063-651X(97)50710-0]

PACS number(s): 05.45.+b, 75.80.+q

Model-independent chaos control techniques, the first of which was developed by Ott, Grebogi, and Yorke [1], have been applied to a wide range of physical and physiological systems [2–11]. Recently, similar techniques have been developed to stabilize underlying unstable periodic orbits (UPO's) in nonchaotic dynamical systems [12–18]. In general, model-independent control techniques use feedback perturbations to stabilize a dynamical system about one of its UPO's. In contrast to traditional control techniques (which require knowledge of a system's governing equations), model-independent techniques are inherently well-suited for ''black-box'' systems because they extract all necessary control information from a premeasured time series. The flexibility of model independence in current dynamical control techniques, however, does not come without limitations. The precontrol time-series measurement and the corresponding system-dynamics estimation comprise a ''learning'' stage. For some real-world systems (e.g., cardiac arrhythmias), however, unwanted dynamics must be eliminated quickly, and thus the time required for a learning stage may be unavailable.

Recently, a real-time, adaptive, model-independent (RTAMI) control technique, was developed [19] to stabilize flip-saddle UPO's in chaotic and nonchaotic dynamical systems that can be described effectively by a unimodal one-dimensional map. Because the RTAMI technique does not require a precontrol learning stage (i.e., it operates in real time) it is practical for on-the-fly control of dynamical systems. In Ref. [19], the RTAMI technique was successfully applied to a wide range of model systems in their nonchaotic and chaotic regimes. Here, we apply the RTAMI control technique to an experimental system — a driven magnetoelastic ribbon — in its nonchaotic and chaotic regimes.

The RTAMI technique is designed to stabilize the flip-saddle unstable periodic fixed point $\boldsymbol{\xi}^*=[x^*,x^*]^T$ (where superscript $T$ denotes transpose and $[x^*,x^*]^T$ is a $2\times1$ column vector) of a system that can be described effectively by a unimodal one-dimensional map $x_{n+1}=f(x_n,p_n)$, where $x_n$ is the current value (scalar) of one measurable system variable, $x_{n+1}$ is the next value of the same variable, and $p_n$ is the value (scalar) of an accessible system parameter $p$ at index $n$. The control technique perturbs $p$ such that $p_n=\overline{p}+\delta p_n$, where $\overline{p}$ is the nominal parameter value, and $\delta p_n$ is a perturbation [3,4,20–22] given by

$$\delta p_n=\frac{x_n-x_n^*}{g_n}, \tag{1}$$

where $x_n^*$ is the current estimate of $x^*$, and $g_n$ is the control sensitivity $g$ at index $n$. The ideal value of $g$ is the sensitivity of $x^*$ to perturbations: $g_{\rm ideal}=\delta x^*/\delta p$. As described in Ref. [23], control can be achieved for nonideal values of $g$ in the range $|g|_{\rm min}\le|g|\le|g|_{\rm max}$. (Prior to control, it is not possible to determine $g_{\rm min}$ or $g_{\rm max}$ without an analytical system model or a learning stage.)

As shown in Fig. 1, the current state point $\boldsymbol{\xi}_n$ would move,

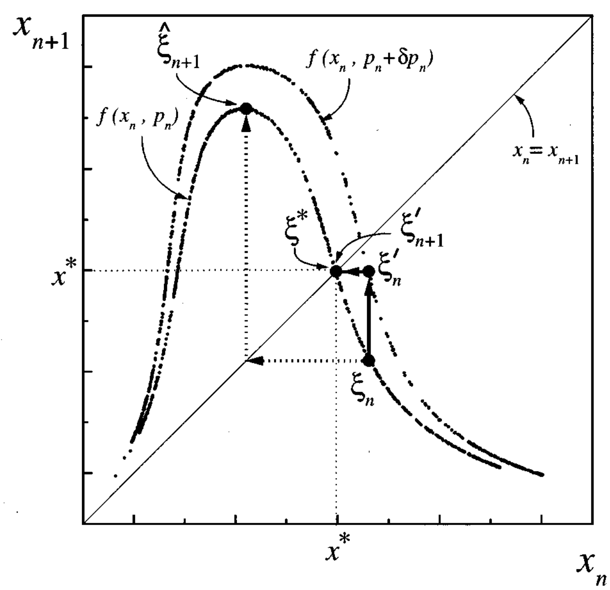


FIG. 1. First-return map showing that $\delta p_n$ [Eq. (1), with $g=g_{\rm ideal}$] shifts the map from $f(x_n,p_n)$ to $f(x_n,p_n+\delta p_n)$ such that the next system state point is forced to $\boldsymbol{\xi}'_{n+1}\approx\boldsymbol{\xi}^*$, rather than to its expected position $\hat{\boldsymbol{\xi}}_{n+1}$. These data, shown for illustrative purposes, are from simulations of the Belousov-Zhabotinsky chemical reaction.

 

in the absence of a perturbation (i.e., $\delta p_n = 0$), to $\hat{\xi}_{n+1}$ (via the dotted arrow). However, the control perturbation of Eq. (1) (corresponding to $g = g_{\mathrm{ideal}}$) shifts $f(x_n, p_n)$ to $f(x_n, p_n + \delta p_n)$ such that $x_n$ maps to $x'_{n+1} = x^*$, instead of $\hat{x}_{n+1}$. On the first-return map, this shift appears as the movement of $\xi_n$ to $\xi'_n$ (via the solid vertical arrow in Fig. 1). When the map is returned to $f(x_n, p_n)$ for the next iteration, the next state point will be $\xi'_{n+1} \approx \xi^*$, as desired for control. In a physical system, due to noise, measurement errors, and the instability of $\xi^*$, perturbations are required at each iteration to hold $\xi_n$ within the neighborhood of $\xi^*$.

Learning-stage dependent techniques use static values for $x^*$ and/or $g$, as estimated from a precontrol time-series measurement. In contrast, the RTAMI technique repeatedly estimates $x^*$ and $g$. In addition to eliminating the need for a learning stage, this adaptability allows for the control of nonstationary systems. When control is initiated, $g$ can be set to an arbitrary value (with the restriction that the sign of $g$ must match that of $g_{\mathrm{ideal}}$; if the signs do not match, control will fail). After each measurement of $x_n$, $x^*$ is estimated using

$$x_n^* = \sum_{i=0}^{N-1} \frac{x_{n-i}}{N}, \tag{2}$$

where $N$ is the number of past data points included in the average [24]. Equation (2) converges to $x^*$ because consecutive $x_n$ alternate on either side of $x^*$ due to the flip-saddle nature of $\xi^*$.

At each iteration, after $x^*$ is re-estimated via Eq. (2), the RTAMI technique evaluates whether the estimate of $g$ should be adapted. The value of $g$ is not adapted if the desired control precision $\epsilon$ has been achieved. Control precision has *not* been achieved if

$$|x_n - x_{n-1}^*| > \epsilon \tag{3}$$

is satisfied by at least $L$ data points out of the $N$ previous data points, where $x_{n-1}^*$ is the estimate of $x^*$ that was targeted for a given $x_n$. The $L/N$ factor is used [instead of a single evaluation of Eq. (3)] to reduce the influence of noise and spurious data points.

If the desired control precision has not been achieved [i.e., Eq. (3) has been satisfied by at least $L$ data points out of the $N$ previous data points], then the magnitude of $g$ is adapted in accordance with the expected perturbation dynamics [19]. If $g = g_{\mathrm{ideal}}$, then the perturbation moves the state point from its current position $\xi_n$ to $\xi^*$ (as in Fig. 1). If $|g|$ is too large (i.e., $\delta p$ is too small), then the state point moves from its current position $\xi_n$ to a position closer to $\xi^*$ than would be expected without a perturbation. If $|g|$ is too small (i.e., $\delta p$ is too large), then the state point moves from its current position $\xi_n$ to a position on the same side of the line of identity. (This is in contrast to the expected alternation, due to the flip-saddle nature of $\xi^*$, of consecutive state points on either side of the line of identity.) The criterion

$$\mathrm{sgn}(x_n - x_{n-1}) = \mathrm{sgn}(x_{n-1} - x_{n-2}) \tag{4}$$

is satisfied when two consecutive state points ($[x_{n-1}, x_{n-2}]$ and $[x_n, x_{n-1}]$) lie on the same side of the line of identity. The RTAMI technique increases the magnitude of $g$ (i.e., $g_{n+1} = g_n \rho$, where $\rho$ is the adjustment factor) if Eq. (4) is satisfied for at least $L$ data points out of the $N$ previous data points. As with the evaluation of control precision [Eq. (3)], the $L/N$ factor is used [instead of a single evaluation of Eq. (4)] to reduce the influence of noise and spurious data points.

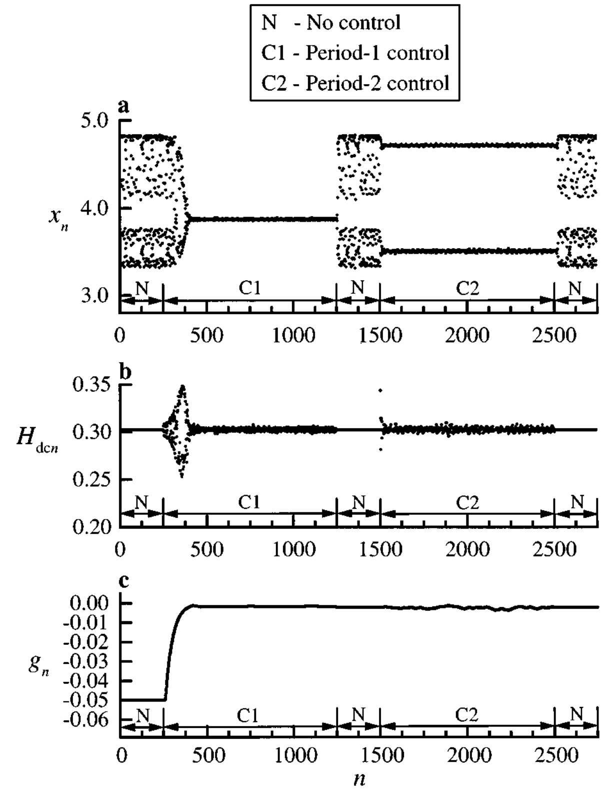


FIG. 2. (a) $x_n$, (b) $H_{\mathrm{dc}n}$, and (c) $g_n$ versus drive cycle $n$ for a RTAMI control trial of the chaotic magnetoelastic ribbon. The respective control stages are annotated in (a), (b), and (c).

If the magnitude of $g$ is not increased [as dictated by Eq. (4)], then the magnitude of $g$ is decreased if $\xi_n$ is not converging rapidly (at a rate governed by $r$) to $\xi^*$. Specifically, the magnitude of $g$ is decreased (i.e., $g_{n+1} = g_n / \rho$) if

$$\frac{1}{N} \sum_{i=0}^{N-1} \frac{|x_{n-i-1} - x_{n-i-2}^*| - |x_{n-i} - x_{n-i-1}^*|}{|x_{n-i-1} - x_{n-i-2}^*|} < r\% . \tag{5}$$

Equation (5) is satisfied if, on average, the distance $|x_{n-i} - x_{n-i-1}^*|$ between a given data point $x_{n-i}$ and its corresponding fixed-point estimate $x_{n-i-1}^*$ is not at least $r\%$ smaller than the distance $|x_{n-i-1} - x_{n-i-2}^*|$ between the previous data point $x_{n-i-1}$ and the previous fixed-point estimate $x_{n-i-2}^*$.

If neither Eq. (4) nor Eq. (5) is satisfied, then $g$ is not adapted because $x$ is properly approaching the estimate of $x^*$.

The experimental system we considered [25] consists of a gravitationally buckled magnetoelastic ribbon driven parametrically by a sinusoidally varying magnetic field. The ribbon is clamped at its lower end and its position $x$ is measured once per drive period at a point a short distance above the clamp. The ribbon's Young's modulus can be varied by applying an external magnetic field. The applied magnetic field

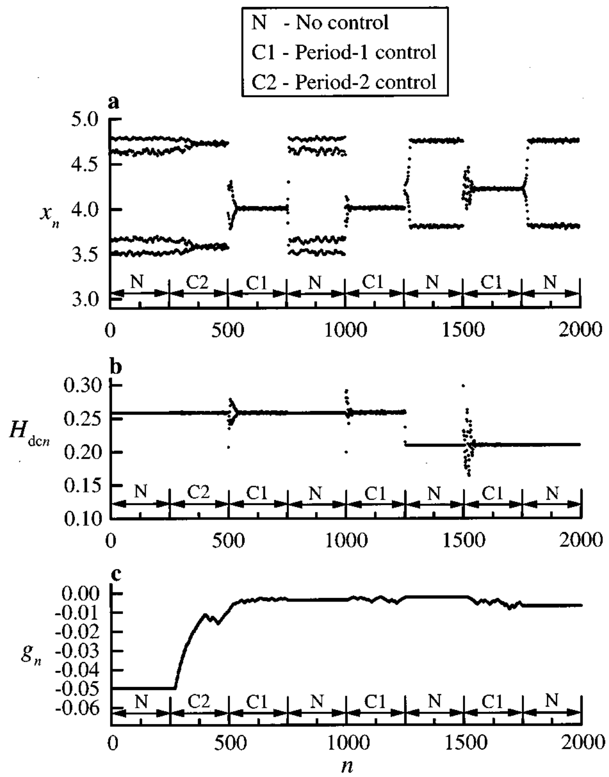


FIG. 3. (a) $x_n$, (b) $H_{dcn}$, and (c) $g_n$ versus drive cycle $n$ for a RTAMI control trial of the magnetoelastic ribbon in two different nonchaotic regimes [stable period-4 regime ($1 \leq n \leq 1250$) and stable period-2 regime ($1250 < n \leq 2000$)].

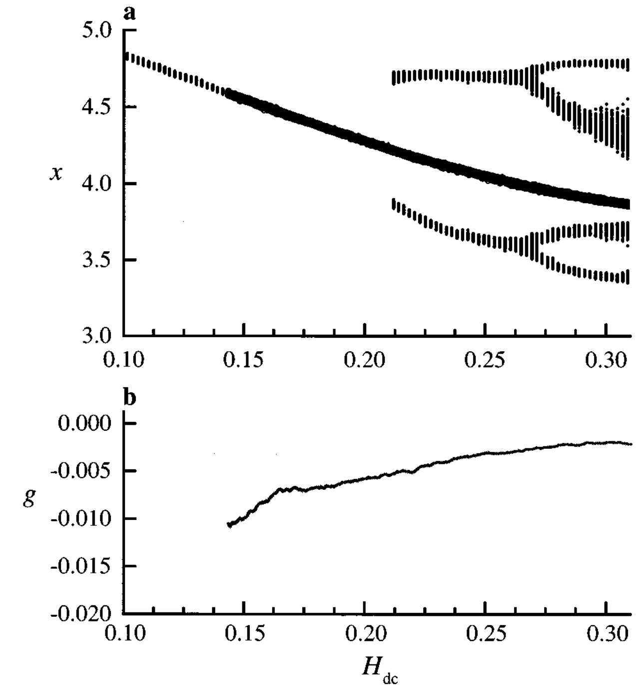


FIG. 4. (a) $x$ versus $H_{dc}$ for a RTAMI tracking trial (dark points) overlaid onto the corresponding bifurcation diagram. (b) $g$ for the tracking trial shown in (a).

is $H_{app} = H_{dc} + H_{ac}\sin(2\pi ft)$, where $H_{dc}$ is the dc-field amplitude, $H_{ac}$ is the ac-field amplitude, and $f$ is the ac-field frequency. To apply the RTAMI control technique to the magnetoelastic ribbon, $H_{dc}$ was used as the control parameter [i.e., $p_n \equiv H_{dcn}$ such that $H_{dcn} = \overline{H_{dc}} + \delta H_{dcn}$].

Figure 2 shows a typical RTAMI control trial (with $\overline{H_{dc}} = 0.302$ Oe, $H_{ac} = 1.037$ Oe, $f = 0.9$ Hz, $N = 10$, $\epsilon = 0.01$, $L = 3$, $r = 5\%$, and $\rho = 1.025$). At $n = 250$, following a period of chaotic ribbon motion (corresponding to a two-piece attractor), control of the unstable period-1 fixed point was activated. The initial control perturbations [Fig. 2(b)] were too small (because $|g|$ was too large) to move the state point into the neighborhood of the fixed point (and hold it within that neighborhood) [Fig. 2(a)]. Thus, $|g|$ was decreased [as dictated by Eq. (5)] until the magnitude of the perturbations increased and the state point converged to the unstable period-1 fixed point. Note that although Eq. (1) is only valid in the linear region of $\xi^*$, the value of $g$ required to pull $\xi_n$ into the neighborhood of $\xi^*$ was also suitable for the stabilization of $\xi^*$ (i.e., $|g|_{min} \leq |g| \leq |g|_{max}$). Also note that it is possible that the large parameter perturbations required to move $\xi_n$ into the neighborhood of $\xi^*$ could alter $p$ to a regime where $\xi^*$ is stable. However, because of the flip-saddle nature of $\xi^*$, consecutive perturbations (excluding those influenced by noise or when $|g|$ is too small) are opposite in polarity, thereby ensuring that a parameter-regime change into the stable regime of $\xi^*$ is followed by a parameter-regime change away from the stable regime of $\xi^*$. Thus, the large perturbations should not be mistaken for a parameter-regime shift that is used to capture $\xi^*$ when it is stable, in order to drag it back into the unstable regime.

Stabilization was maintained until $n = 1250$, when control was deactivated. At $n = 1500$, stabilization of the system's unstable period-2 fixed point was activated [26]. Period-2 stabilization was quickly achieved by updating the estimates for $x_n^*$ and $g$ and applying control interventions at every other iterate rather than at every iterate.

Figure 3 shows a RTAMI control trial (with $\overline{H_{dc}} = 0.258$ Oe, $H_{ac} = 1.037$ Oe, $f = 0.9$ Hz, $N = 10$, $\epsilon = 0.00$ [27], $L = 3$, $r = 5\%$, and $\rho = 1.025$) that demonstrates: (i) on-the-fly control of a system that is switched rapidly between different parameter regimes and (ii) stabilization of UPO's which underlie stable higher-period orbits in a nonchaotic system. At $n = 250$, following a period of stable period-4 ribbon oscillation, control of the system's underlying unstable period-2 fixed point was activated. After $|g|$ was decreased, as dictated by Eq. (5), period-2 stabilization was achieved and maintained until $n = 500$, when the control target was switched from the underlying unstable period-2 fixed point to the underlying unstable period-1 fixed point. Period-1 stabilization was maintained until $n = 750$, when control was deactivated. At $n = 1000$, period-1 stabilization was reactivated directly from the stable period-4 oscillation. Period-1 stabilization was maintained until $n = 1250$, when control was deactivated and $\overline{H_{dc}}$ was changed to $\overline{H_{dc}} = 0.210$ Oe, corresponding to a stable period-2 oscillation. At $n = 1500$, period-1 stabilization was activated directly from the stable period-2 oscillation. Note that the magnitude of $g$ increased and decreased [Fig. 3(c)], as dictated by Eqs. (4) and (5), for the different unstable periodic fixed points and parameter regimes.

In addition to controlling a dynamical system in its nonchaotic or chaotic regimes, the RTAMI technique is capable of "tracking" [12–16,22] an unstable periodic fixed point from its stable period-1 regime through multiple period-doubling bifurcations into the chaotic regime, and vice versa (i.e., from its chaotic regime back to its stable period-1 regime). Figure 4 shows a tracking trial in which the RTAMI technique was used (with $H_{ac}=1.037$ Oe, $f=0.9$ Hz, $N=10$, $\epsilon=0.00$, $L=3$, $r=5\%$, and $\rho=1.001$) to track the unstable period-1 fixed point from $\overline{H}_{dc}=0.311$ Oe (chaotic regime) to $\overline{H}_{dc}=0.144$ Oe (stable period-1 regime). Figure 4(a) shows the tracking trial (dark points) overlaid onto the corresponding bifurcation diagram, while Fig. 4(b) shows the corresponding $g$. Note that $|g|$ was largest (i.e., most negative) when the slope $\delta x/\delta H_{dc}$ of the period-1 fixed point in Fig. 4(a) was largest, and $|g|$ was smallest (i.e., least negative) when the slope $\delta x/\delta H_{dc}$ of the period-1 fixed point was smallest. This further demonstrates (because $g_{ideal}=\delta x/\delta H_{dc}$) that the RTAMI technique effectively adapts $g$.

The RTAMI control technique was unable to stabilize the unstable period-1 fixed point of the driven magnetoelastic ribbon in the chaotic parameter regime $\overline{H}_{dc}>0.311$ Oe. This control failure resulted from the fact that the value of $g$ required initially to move $\xi_n$ into the neighborhood of $\boldsymbol{\xi}^*$ was not within the range of $g$ values suitable for stabilizing $\boldsymbol{\xi}^*$. This is in contrast to the case where $\overline{H}_{dc}<0.311$ Oe (as described for Fig. 2) in which the value of $g$ required to pull $\boldsymbol{\xi}_n$ into the neighborhood of $\boldsymbol{\xi}^*$ was suitable for control (i.e., $|g|_{min}\leq|g|\leq|g|_{max}$). When $\overline{H}_{dc}>0.311$ Oe, $|g|<|g|_{min}$ was required to pull $\boldsymbol{\xi}_n$ into the neighborhood of $\boldsymbol{\xi}^*$. Thus, once $\boldsymbol{\xi}_n$ entered the neighborhood of $\boldsymbol{\xi}^*$, oversized perturbations [28] were delivered that promptly repelled $\boldsymbol{\xi}_n$ from $\boldsymbol{\xi}^*$ before the magnitude of $g$ could be increased.

In this paper, we have shown that the RTAMI technique can be used to control an experimental system. Specifically, we have controlled the motion of a driven magnetoelastic ribbon in its period-2 regime, period-4 regime, and chaotic regime. We have demonstrated that the RTAMI control technique is capable of (i) on-the-fly control as a system is switched between parameter regimes, (ii) stabilizing higher-order UPO's, and (iii) tracking a UPO through multiple bifurcations. These results demonstrate that the RTAMI technique is versatile and practical for real-time control of real-world systems.

This work was supported by the National Science Foundation (D.J.C., J.J.C.), the ONR/ASEE Postdoctoral Fellowship Program (V.I.), the Office of Naval Research Physical Sciences Division (M.L.S., W.L.D.), and the NSWC Independent Laboratory Internal Research Program (M.L.S.).

[1] E. Ott, C. Grebogi, and J. A. Yorke, Phys. Rev. Lett. **64**, 1196 (1990).
[2] W. L. Ditto, S. N. Rauseo, and M. L. Spano, Phys. Rev. Lett. **65**, 3211 (1990).
[3] E. R. Hunt, Phys. Rev. Lett. **67**, 1953 (1991).
[4] B. Peng, V. Petrov, and K. Showalter, J. Phys. Chem. **95**, 4957 (1991).
[5] R. Roy, T. W. Murphy, Jr., T. D. Maier, Z. Gills, and E. R. Hunt, Phys. Rev. Lett. **68**, 1259 (1992).
[6] P. Parmananda, P. Sherard, R. W. Rollins, and H. D. Dewald, Phys. Rev. E **47**, R3003 (1993).
[7] V. Petrov, V. Gáspár, J. Masere, and K. Showalter, Nature (London) **361**, 240 (1993).
[8] B. Hübinger, R. Doerner, W. Martienssen, W. Herdering, R. Pitka, and U. Dressler, Phys. Rev. E **50**, 932 (1994).
[9] D. J. Christini, J. J. Collins, and P. S. Linsay, Phys. Rev. E **54**, 4824 (1996).
[10] A. Garfinkel, M. L. Spano, W. L. Ditto, and J. N. Weiss, Science **257**, 1230 (1992).
[11] S. J. Schiff, K. Jerger, D. H. Duong, T. Chang, M. L. Spano, and W. L. Ditto, Nature (London) **370**, 615 (1994).
[12] T. L. Carroll, I. Triandaf, I. Schwartz, and L. Pecora, Phys. Rev. A **46**, 6189 (1992).
[13] Z. Gills, C. Iwata, R. Roy, I. B. Schwartz, and I. Triandaf, Phys. Rev. Lett. **69**, 3169 (1992).
[14] I. B. Schwartz and I. Triandaf, Phys. Rev. A **46**, 7439 (1992).
[15] I. Triandafand I.B. Schwartz, Phys. Rev. E **48**, 718 (1993).
[16] V. Petrov, M. J. Crowley, and K. Showalter, Phys. Rev. Lett. **72**, 2955 (1994).
[17] D. J. Christini and J. J. Collins, Phys. Rev. E **52**, 5806 (1995).
[18] D. J. Christini and J. J. Collins, Phys. Rev. E **53**, R49 (1996).
[19] D. J. Christini and J. J. Collins, IEEE Trans. Circuits Syst. (to be published).
[20] V. Petrov, B. Peng, and K. Showalter, J. Chem. Phys. **96**, 7506 (1992).
[21] K. Pyragas, Phys. Lett. A **170**, 421 (1992).
[22] D. J. Gauthier, D. W. Sukow, H. M. Concannon, and J. E. S. Socolar, Phys. Rev. E **50**, 2343 (1994); J. E. S. Socolar, D. W. Sukow, and D. J. Gauthier, *ibid.* **50**, 3245 (1994).
[23] K. Hall, D. J. Christini, M. Tremblay, J. J. Collins, L. Glass, and J. Billette, Phys. Rev. Lett. **78**, 4518 (1997).
[24] G. W. Flake, G.-Z. Sun, Y.-C. Lee, and H.-H. Chen, in *Advances in Neural Information Processing*, edited by J. D. Cowan, G. Tesauro, and J. Alspector (Morgan Publishers, San Mateo, CA, 1994), p. 647.
[25] W. L. Ditto, S. Rauseo, R. Cawley, C. G. G. H. Hsu, E. Kostelich, E. Ott, H. T. Savage, R. Segnam, M. L. Spano, and J. A. Yorke, Phys. Rev. Lett. **63**, 923 (1989).
[26] Period-2 control can fail for systems which have two unstable period-2 fixed points that are characterized by $g$'s with opposite signs. In such systems, failure will occur if the initial value of $g$ for the targeted fixed point has the sign corresponding to $g$ for the other fixed point.
[27] Setting $\epsilon=0.00$ is equivalent to eliminating Eq. (3) from the RTAMI algorithm. This simplifies the real-world applicability of the technique by eliminating a parameter (i.e., $\epsilon$).
[28] The perturbations were oversized because $|g|$ was too small for the neighborhood of the fixed point. This resulted in consecutive state points that were forced onto the same side of the line of identity.